

The relationship between the eddy-driven jet stream and northern European sea level variability

By FABIO MANGINI^{1*}, LÉON CHAFIK², ERICA MADONNA³, CAMILLE LI³, LAURENT BERTINO¹, and JAN EVEN ØIE NILSEN^{1,4}, ¹*Nansen Environmental and Remote Sensing Center and Bjerknes Centre for Climate Research, Bergen, Norway;* ²*Department of Meteorology and Bolin Centre for Climate Research, Stockholm University, Stockholm, Sweden;* ³*Geophysical Institute and Bjerknes Centre for Climate Research, University of Bergen, Bergen, Norway;* ⁴*Institute of Marine Research, Bergen, Norway*

(Manuscript Received 14 July 2020; in final form 22 January 2021)

ABSTRACT

Wintertime sea level variability over the northern European continental shelf is largely wind-driven. Using daily gridded sea level anomaly from altimetry, we examine both the spatial and the temporal relationship between northern European sea level variability and large-scale atmospheric circulation patterns as represented by the jet cluster paradigm. The jet clusters represent different configurations of the eddy-driven jet stream and, therefore, provide a physical description of the atmospheric variability in the North Atlantic. We find that each of the four jet clusters is associated with a distinct northern European sea level anomaly pattern whose magnitudes are comparable to those of typical sea level variations on the shelf. In certain locations, such as the German Bight and the east coast of England, sea level anomalies are mainly associated with one single jet cluster. In other locations, such as the interior and the northern part of the North Sea, sea level anomalies are found to be sensitive to at least two jet configurations. Based on these regional sea level variations, we map out the locations on the shelf where each jet cluster or combination of clusters is most active before discussing the role of Ekman transport in inducing the resulting patterns. Through a multiple linear regression model, we also find that the jet clusters reconstruct up to 50% of the monthly mean sea level anomaly variance over the northern European continental shelf. The model best performs in the interior and the western part of the North Sea, suggesting that wind direction rather than wind speed plays a more prominent role over these regions. We conclude that the jet cluster approach gives valuable new insights compared to linear regression techniques for characterising wind-driven sea level variability over the northern European continental shelf.

Keywords: northern European sea level, jet clusters, wind forcing, eddy-driven jet stream, satellite altimetry

1. Introduction

Local winds contribute to sea level variability over the northern European continental shelf from hourly up to interannual timescales. At timescales shorter than a few days, local winds can generate storm surges that severely affect the coastal regions of northern Europe, most of which are low-lying and densely populated (e.g. Wahl et al., 2013; Gill, 1982; Lamb and Frydendahl, 1991). At longer timescales, they modify the height and frequency of storm surges and partly explain the departure of northern European sea level rise from the global average (e.g. Dangendorf et al., 2012). An in-depth knowledge of sea level variations at different timescales would thus

benefit both climate scientists in understanding the processes involved and coastal planners in decision making.

Previous studies showed a relationship between northern European sea level and the North Atlantic Oscillation (NAO), the leading mode of atmospheric variability over the North Atlantic (e.g. Wakelin et al., 2003; Yan et al., 2004; Jevrejeva et al., 2005; Richter et al., 2012). The NAO is a simple index that allows for a compact description of North Atlantic atmospheric conditions (e.g. Hurrell, 1995) and, as such, has been widely used in the past to investigate the variability of the climate system. It has been found that the positive and the negative phases of the NAO are, respectively, associated with high and low sea level over the entire northern European continental shelf (e.g. Wakelin et al., 2003; Richter et al., 2012;

*Corresponding author. e-mail: fabio.mangini@nersc.no

Chafik et al., 2017). Moreover, the sea level variability connected to the NAO has been found to be strongest at annual and interannual timescales (e.g. Yan et al., 2004) and in specific locations such as the southern North Sea (e.g. Wakelin et al., 2003).

There remains, however, a substantial portion of North Atlantic atmospheric variability that is unrelated to the NAO, and this has been found to contribute to the spatial and the temporal sea level variability over the northern European continental shelf. For example, Chafik et al. (2017) showed that additional patterns of atmospheric variability, defined via empirical orthogonal function (EOF) analysis, contribute significantly to regional sea level variations across the North Sea and the Norwegian shelf. Dangendorf et al. (2014) focused on one region, the German Bight, and built a bespoke atmospheric index to reproduce the contribution of both wind and pressure to the sea level. Their index explains $\sim 80\%$ of the sea level variance at this specific location, compared to 30–35% from a standard NAO index. In summary, sea level variability may be better explained by accounting for atmospheric variability beyond the NAO.

While these approaches give insight into wind-driven sea level variability, there is some uncertainty as to whether the wind patterns they identify correspond to real (observed) large-scale atmospheric conditions. EOFs must satisfy symmetry and orthogonality constraints and, therefore, do not necessarily describe patterns that occur in nature. Moreover, the method proposed by Dangendorf et al. (2014) yields only one atmospheric pattern associated with either high or low sea level values at one selected location. Therefore, their approach is not designed to identify the atmospheric conditions responsible for coherent sea level patterns over a large area like the northern European continental shelf.

Here, we study how northern European sea level variability relates to wind patterns using the jet cluster paradigm (Madonna et al., 2017), an approach that provides a physical description of large-scale atmospheric variability and has so far not been used in sea level research. The jet clusters represent observed configurations of the eddy-driven jet stream which are associated with a set of well-known weather regimes that characterise Euro-Atlantic climate. We start with a brief description of the datasets used (Section 2). We then describe the sea level patterns associated with the jet clusters and explore where the jet clusters account for a substantial portion of the interannual sea level variability (Section 3). We discuss the balance of forces on the shelf and the role of Ekman transport as a mechanism for creating the observed sea level patterns (Section 4). We then examine how the jet clusters and

the northern European sea level co-vary at daily and monthly time scale (Section 5) and conclude with some final remarks (Section 6).

2. Data

2.1. Time-mean barotropic circulation on the shelf

We use the barotropic streamfunction (ψ) from the TOPAZ4 ocean reanalysis (Xie et al., 2017) to derive the barotropic currents over the northern European continental shelf and parts of the Nordic Seas. The dataset is provided daily from 01 January 1991 and covers the North Atlantic and the Arctic oceans on a Cartesian grid of $0.25^\circ \times 0.25^\circ$. The ocean model data is only used for illustration of the current patterns.

To calculate the time-mean barotropic circulation, we first select the period between 01 January 1993 and 31 December 2014, common to the time series of the sea level anomaly and of the jet clusters (see Sections 2.2 and 2.4). Then, we remove the linear trend and the seasonal cycle (daily climatology) from the barotropic streamfunction, and we average the result over the period under consideration. Finally, we compute the time-mean barotropic current using the formula:

$$u = -\frac{1}{H} \frac{\partial \psi}{\partial y}; \quad v = \frac{1}{H} \frac{\partial \psi}{\partial x} \quad (1)$$

where u and v are the zonal and meridional components of the currents, and H is the ocean depth.

In Fig. 1A, we recognise the main features of the time-mean barotropic circulation over the northern European continental shelf and the Nordic Seas. Along the northern European continental slope, we identify the slope current which flows northward at a speed of a few cm s^{-1} . In the North Sea, we recognise the Dooley current, which follows the 100m isobath, and the coastal current, which flows along the southern coast of the North Sea. Both cross the North Sea from west to east and converge into the Skagerrak. From the Skagerrak, the flow continues northward in the Norwegian Trench along the Norwegian coast as the Norwegian Coastal Current. This description of the main ocean currents on the shelf will be helpful in the discussion later in the study.

2.2. Sea level

We use the absolute dynamic topography (ADT), which is the sea surface height relative to the geoid, of the DUACS reprocessed multi-mission altimetry products DT2014 version (Pujol et al., 2016). The ADT is provided daily from 01 January 1993 and globally on a Cartesian grid of $0.25^\circ \times 0.25^\circ$. A number of geophysical corrections have been

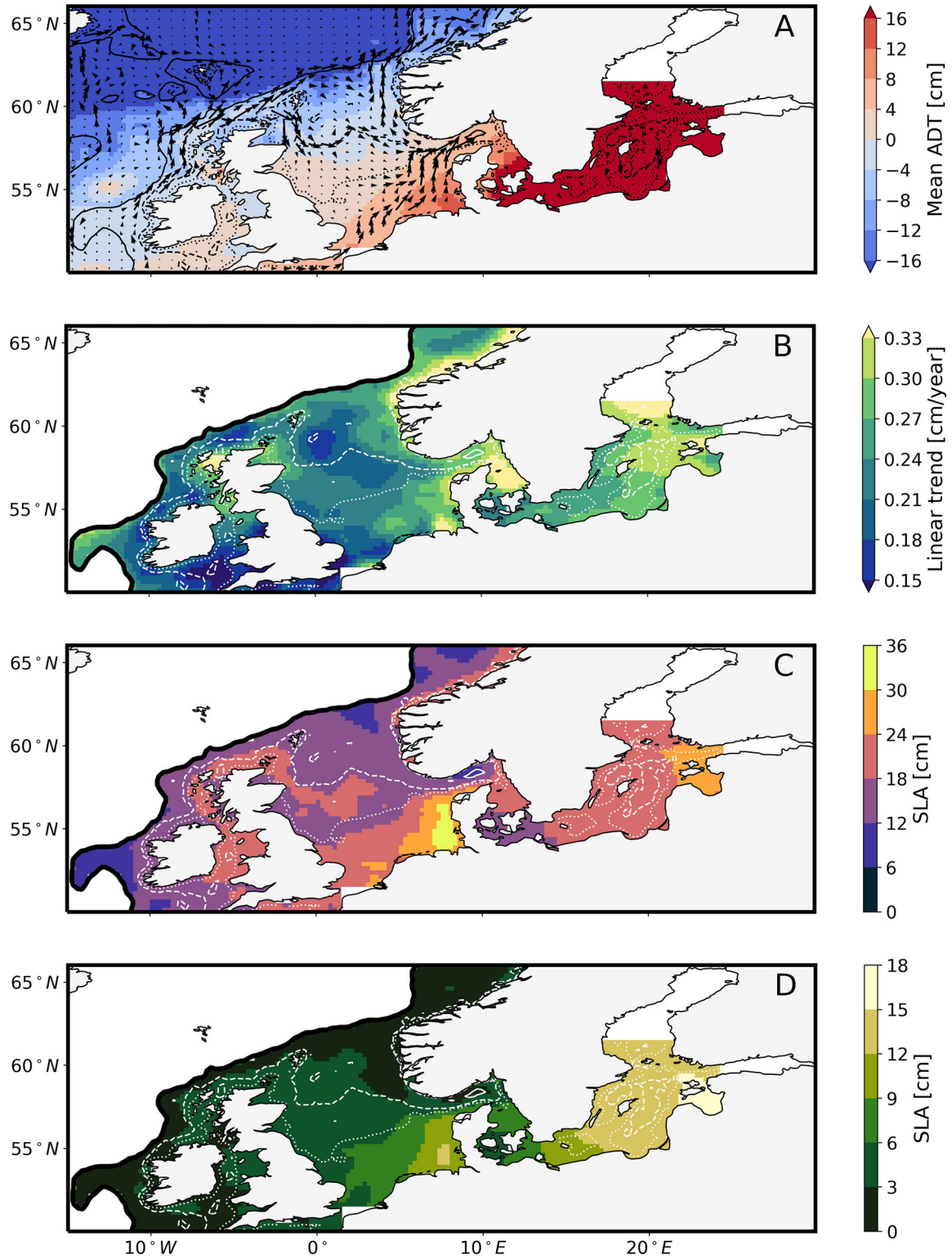


Fig. 1. Spatial sea level statistics from satellite altimetry: (A) annual mean absolute dynamic topography (shading, in cm) over the 1993–2014 period, (B) linear trend (cm/year), (C) range of the seasonal cycle of the sea level anomaly (cm), and (D) standard deviation of the winter-mean sea level anomaly, after removing the linear trend and the seasonal cycle (cm). Mean depth-averaged current from the TOPAZ4 reanalysis (arrows, in m s^{-1}) over the 1993–2014 period (A). The solid/dashed/dotted black/white lines indicate the 500 m/100 m/ 50 m isobaths, respectively. In B, C and D, the grid points over the open ocean are masked and the continental shelf is delimited by the thick black line.

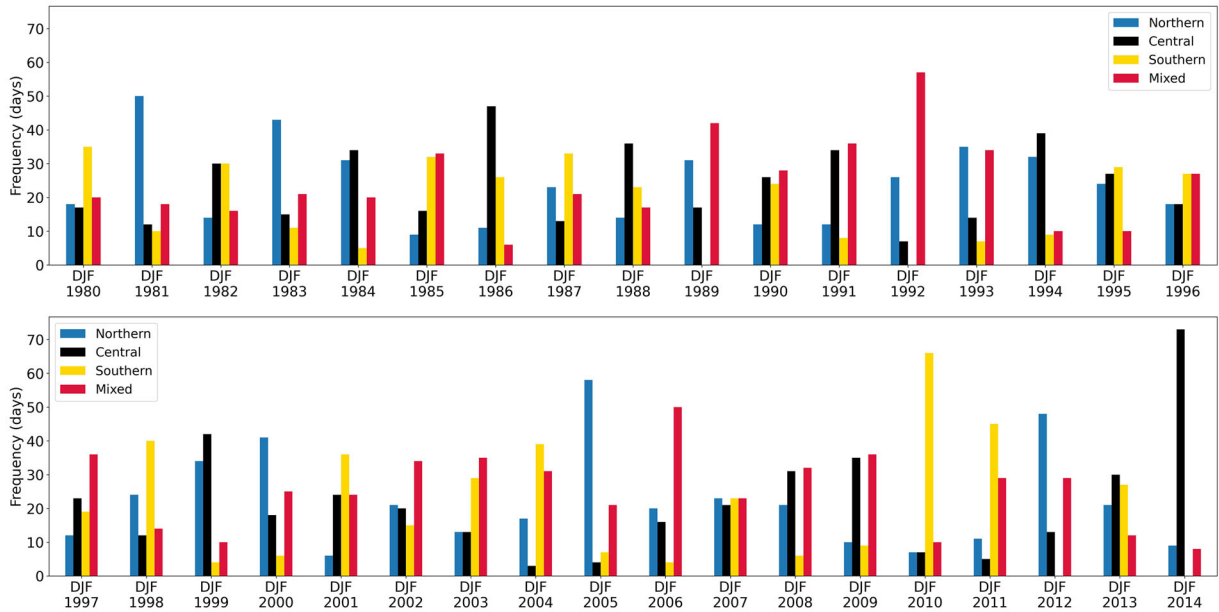


Fig. 2. Frequency (in days) of the jet clusters for each winter between December 1979 and February 2014.

applied to the altimetry data, such as the removal of astronomical tides and the inverse barometer effect, which is the pressure contribution to sea level. Sea level variability with periods shorter than 20 days has been removed as it may lead to aliasing of the satellite data.

We use the ADT to calculate the sea level anomaly (SLA), which is the sea surface height relative to the time-mean (1993–2014) sea level. We focus on the period between January 1993 and December 2014 for the ADT time series to overlap with that used for the calculation of the jet clusters (see Section 2.4). The domain of interest is 15°W – 30°E and 50°N – 66°N (Fig. 1), which includes the northern European continental shelf and parts of the Nordic Seas (the region located north of the northern European continental slope). To calculate the SLA, we remove the average of the daily ADT over the 21-year period between January 1993 and December 2014 at each grid point within the domain (Fig. 1A). We exclude all grid points whose time series of the ADT have gaps, most of which are concentrated in the northern part of the Baltic Sea and the Gulf of Finland, and appear in white in the figures below. Next, we remove the linear trend (Fig. 1B) and seasonal cycle (daily climatology; Fig. 1C). As a measure of the interannual variability of the winter SLA, which is the season of interest in this study, we also show the standard deviation of the winter-mean (December to February) SLA, after removing both the linear trend and the seasonal cycle (Fig. 1D).

Briefly, we note that the mean ADT (Fig. 1A) shows a meridional gradient in the North Sea (with values of -12 cm near the northern boundary and values of 4 cm in the south)

and a zonal gradient in the southern part of the North Sea (with values ranging from approximately 4 cm in the southwest to 16 cm in the German Bight). Trends in sea level (Fig. 1B) are on the order of 1.5 to 3.3 mm year^{-1} , with the highest values being comparable to global mean sea level trends (Cazenave et al., 2018). The range of the seasonal cycle in ADT (Fig. 1C) depends strongly on the considered region, with smaller variations ($\sim 15\text{ cm}$) close to the continental slope and larger variations (~ 20 – 30 cm) over the rest of the continental shelf. Finally, the standard deviation of the winter-mean SLA (Fig. 1D) ranges from 0 to 18 cm and has its minimum in the Norwegian Trench and the Norwegian shelf, and its maximum in the German Bight and the Baltic Sea.

2.3. Atmospheric data

We use the daily 10 m wind and mean sea level pressure (MSLP) fields from the ERA-Interim reanalysis dataset (Dee et al., 2011) of the European Centre for Medium-Range Weather Forecast (ECMWF) with a spatial resolution of $0.75^{\circ} \times 0.75^{\circ}$. We focus on the North Atlantic-European sector and December–January–February (DJF) winter seasons between 1993 and 2014 (21 winters in total) to overlap with the time period over which the jet clusters are calculated (see Section 2.4). Anomalies are calculated for all fields by removing the linear trend and the seasonal cycle (daily climatology).

We also use surface wind stress from satellite scatterometers merged with the ERA-Interim 6-hourly reanalysis dataset (Bentamy et al., 2017). Data are provided at a spatial resolution of $0.25^{\circ} \times 0.25^{\circ}$ from January 1992

onwards. This dataset provides more reliable wind stress values over the northern European continental shelf compared to ERA-Interim, which tends to underestimate wind speeds associated with winter storms (A. Bentamy, personal communication). Similar to the 10m wind and MSLP fields, we remove the linear trend and seasonal cycle (daily climatology) from the wind stress, and we consider only the winter seasons between December 1993 and February 2014.

The surface wind stress dataset contains gaps over the ocean west of the prime meridian. At any grid point, the gaps jointly comprise less than 20% of the days between January 1993 and December 2014, and mainly occur between 1996 and 2001. The presence of the gaps is a source of error for Fig. 6 (see Section 4) since it creates a band of anomalously high/low rate of change of the sea level along the prime meridian. Therefore, to produce Fig. 6, we identify and exclude all the days when the number of gaps over the ocean was anomalously high.

2.4. Jet clusters

We classify the winter-time large-scale variability of the atmosphere according to four North Atlantic jet clusters (Madonna et al., 2017). The jet clusters represent different configurations of the eddy-driven jet stream: northern (N), central (C), southern (S), and ‘mixed’ (split or strongly tilted; M). They are defined from the daily low-pass filtered zonal wind field between 900 and 700 hPa over the North Atlantic (60°W–0°, 15°N–75°N) using a k-mean clustering algorithm (see details in Madonna et al., 2017) and correspond directly to the four classical Euro-Atlantic weather regimes (e.g. Vautard, 1990; Michelangeli et al., 1995).

The relationship between the jet clusters and the weather regimes gives confidence that the jet clusters represent physical states of the atmosphere. Previous studies (e.g. Michelangeli et al., 1995; Cassou et al., 2011; Barrier et al., 2013, 2014) confirmed that the same North Atlantic regimes emerge robustly when the analysis is repeated with different variables (e.g. MSLP, 500 hPa geopotential height), different methods (e.g. k-mean clustering, hierarchical clustering), and different reanalysis products covering different periods. A sufficiently long record is needed, however, to properly sample the large internal variability of the atmosphere, especially in the largely eddy-driven North Atlantic sector (Li and Wettstein, 2012). Therefore, to calculate the jet clusters, we use 35 winters from 01 December 1979 to 28 February 2014 (as in Madonna et al., 2017), even if for sea level analysis we only consider the period starting from December 1993. Even though the frequency of occurrence exhibits a large interannual variability (Fig.

2), we expect not to under-represent any jet cluster by selecting this period of time. Indeed, the jet clusters occur with similar frequency over the periods 1993–2014, 1979–1993 and 1979–2014 (Table 1), in agreement with Madonna et al. (2019) (their Fig. 6). When compared to the NAO, Madonna et al. (2017) showed that the negative phase of the NAO resembles the Southern jet cluster, whereas the positive phase of the NAO does not clearly relate to any jet cluster and, therefore, corresponds to different jet configurations.

Figure 3 shows composites of the daily 10 m wind and MSLP anomalies for each jet cluster. The Northern jet cluster (Fig. 3N, blue frame) is characterised by a zonal eddy-driven jet stream directed towards Scandinavia (contours at ~55°N) and a MSLP dipole with positive values over the subpolar gyre and negative values over the Nordic Seas. During Central jet cluster events (Fig. 3C, black frame), the eddy-driven jet stream is located at ~45°N, directed towards France and the UK, with a low MSLP anomaly over the North East Atlantic and the North Sea. The Southern jet cluster (Fig. 3S, yellow frame) has a zonally oriented eddy-driven jet stream located at approximately 35°N over the mid-latitude North Atlantic and is characterised by an atmospheric high pressure anomaly over Greenland. The Mixed jet cluster (Fig. 3M, red frame) is characterised by a split or strongly tilted jet stream. Its main features are strong westerly winds over the Nordic Seas and a high pressure anomaly over northern and central Europe that is linked to Scandinavian blocking (Madonna et al., 2017).

3. Spatial relationship between the northern European sea level and the jet clusters

3.1. Sea level patterns and jet clusters

Each jet cluster is associated with a distinct sea level pattern over the northern European continental shelf (Fig. 4). We identify each pattern through composite analysis, by averaging the SLA over all the days of occurrence of each jet cluster. This approach does not account for the time needed for the sea level to adjust to variations in the wind field and, therefore, does not consider that the sea level pattern over the northern European continental shelf might not be representative of the dominant jet cluster during its first few days of occurrence. To check whether this might affect the results in Fig. 4, we repeat the composite maps, this time selecting only those cases when the jet clusters persist for four days or longer (Fig. S1). We find that the results in Fig. 4 are robust. In fact, Fig. S1 shows the same patterns as in Fig. 4, but the former are slightly more pronounced than the latter (by 1 to 2 cm).

Table 1. Frequency of occurrence of each jet cluster over the entire period considered (December 1979–February 2014), between December 1979 and February 1993 and over the period covered in the paper (December 1993 and February 2014).

	December 1979–February 2014	December 1979–February 1993	December 1993–February 2014
Northern jet cluster	~25%	~26%	~25%
Central jet cluster	~25%	~25%	~25%
Southern jet cluster	~22%	~19%	~23%
Mixed jet cluster	~28%	~29%	~27%

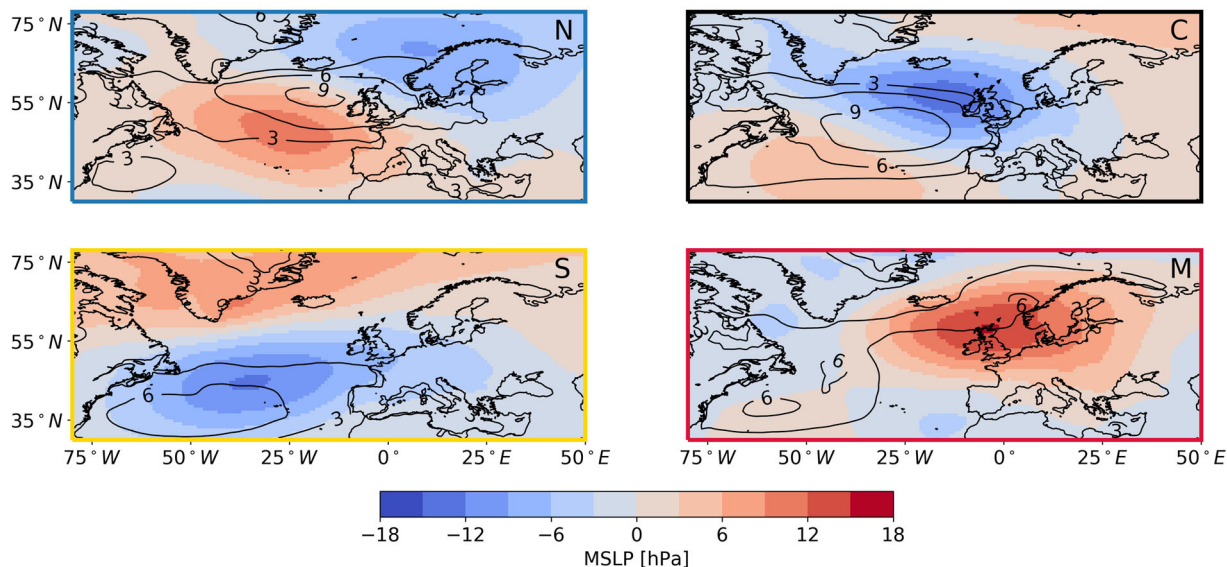


Fig. 3. Composite maps of daily mean sea level pressure anomaly (shading, in hPa) and 10m zonal winds (black contours, 3 m s^{-1} intervals from 3 m s^{-1}) for each jet cluster: (N) Northern jet cluster, (C) Central jet cluster, (S) Southern jet cluster, (M) Mixed jet cluster.

The sea level patterns associated with the jet clusters are particularly strong in the North Sea and the Baltic Sea. In the German Bight and the Baltic Sea, extremely low SLA values (less than -8 cm) are associated with the Southern jet cluster, whereas, along the east coast of England, they are associated with the Central jet cluster. Extremely high SLA values (exceeding 8 cm) are also found in the German Bight and the Baltic Sea, but are associated with the Northern jet cluster. Over the rest of the North Sea, anomalous sea level values are not related to one single jet cluster: negative SLA values are associated with both the Southern and the Central jet clusters, whereas positive SLA values are associated with both the Northern and the Mixed jet clusters. We note that the lowest (-6 cm circa) and the highest (6 cm circa) SLA values in the middle and the northern part of the North Sea are associated with the Central and Mixed jet cluster, respectively.

Sea level anomalies over the Norwegian shelf are generally small compared to the rest of the study area. This is to be expected to some extent, as the Norwegian shelf also exhibits a weaker seasonal cycle

(Fig. 1C) and weak overall sea level variability (Fig. 1D, see also Section 3.2). In fact, SLA is statistically different from zero (at a 0.05 significance level) only for the Southern jet cluster. Despite it being relatively small, the SLA pattern associated with the Southern jet cluster is still of interest since it is comparable in magnitude to the interannual SLA variability over the Norwegian shelf (Fig. 1D), meaning that the Southern jet cluster contributes meaningfully to the interannual SLA variability in the region.

The amplitude of the SLA patterns associated with each jet cluster is smaller but not negligible relative to the amplitude of the seasonal cycle, which is one of the most pronounced features of sea level variability (Fig. 1C). In fact, the magnitude of the SLA associated with the Northern and the Southern jet clusters is approximately one fourth the amplitude of the seasonal cycle in the southern North Sea and approximately one third in the Baltic Sea. Similarly, in the southwest part of the North Sea, the SLA associated with the Central jet cluster is up to one third the amplitude of the seasonal cycle. Therefore, the wind-driven sea level variability associated

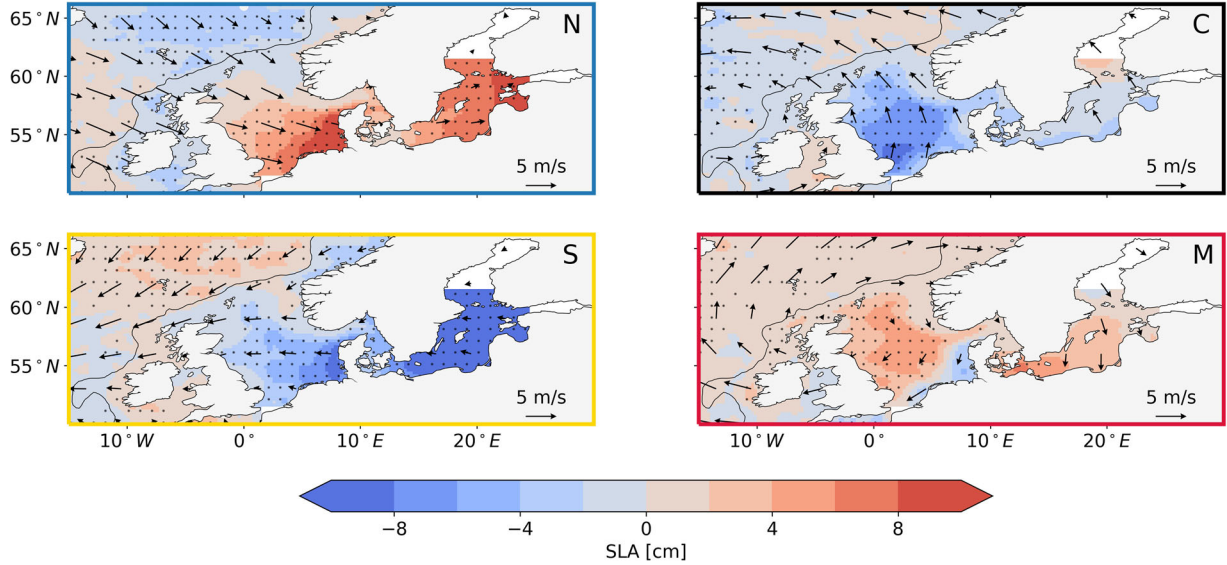


Fig. 4. Composite maps of daily sea level anomaly (shading, in cm) and 10m wind anomaly (arrows, in m s^{-1}) for each jet cluster: (N) Northern jet cluster, (C) Central jet cluster, (S) Southern jet cluster, (M) Mixed jet cluster. The black dots denote regions where the sea level anomaly composite is significantly different from zero at a 0.05 significance level. The grey line shows the location of the continental slope, depicted by the 500m isobath.

with the jet clusters accounts for interannual variability of the seasonal cycle in sea level over a large portion of the northern European shelf, which, in turn, can affect both the height and frequency of occurrence of storm surges in the region (Dangendorf et al., 2012).

Finally, a longer term perspective shows that the SLA patterns associated with the jet clusters are of the same order of magnitude as the sea level rise from 1993 to 2014. Indeed, over the period considered, northern European sea level has risen from approximately 3 cm in the northern North Sea up to 6 cm in the Baltic Sea and the German Bight (Fig. 1B). A comparison between Figs. 1B and 4 can help identify the regions of the shelf where the computed rate of change of sea level is most subject to errors. For example, the error associated with the rate of sea level change is likely to be higher for the southern Baltic Sea and the interior of the North Sea than over the Norwegian shelf. Indeed, compared to the former regions, the latter experiences a similar sea level trend but a weaker atmospheric component of the sea level variability.

3.2. Variability in jet-based sea level anomalies

To better identify the locations of the northern European continental shelf where the SLA variability is most strongly associated with the jet clusters, we compare the composite maps of the SLA (Fig. 4) to a measure of total sea level variability on the shelf. At each grid point, we standardise the composite map of the SLA associated

with each jet cluster (\overline{SLA}_{jc}) by dividing it by the standard deviation of the daily SLA over the 21-winter record (s_{SLA}):

$$\frac{\overline{SLA}_{jc}}{s_{SLA}} \quad (2)$$

When complemented with Fig. 4, Fig. 5 helps identify smaller scale features in the sea level patterns associated with the Northern, the Central, and the Southern jet clusters. From Fig. 5, we learn that the Northern jet cluster explains a higher fraction of the SLA variability in the German Bight than in the Baltic Sea, despite the corresponding composite values of the SLA exceeding 8 cm in both regions (Fig. 4). In addition, we note that, for the Northern jet cluster, the standardised SLA does not significantly change in the southern North Sea, meaning that the Northern jet cluster describes a similar fraction of the SLA variability in the region, even though the composite of the SLA shows lower values along the coast of England than in the German Bight. From Fig. 4, we also know that the lowest sea level values (< -8 cm) occur along the east coast of England during Central jet cluster events, and in the German Bight and the Baltic Sea during Southern jet clusters events. However, when we compare the corresponding standardised values of the SLA, we note that the Central jet cluster describes a larger fraction of the SLA than the Southern jet cluster (the Central jet cluster explains more than 70% of the variability there). In addition, we also note that, opposite to the Northern jet cluster, the Southern jet cluster

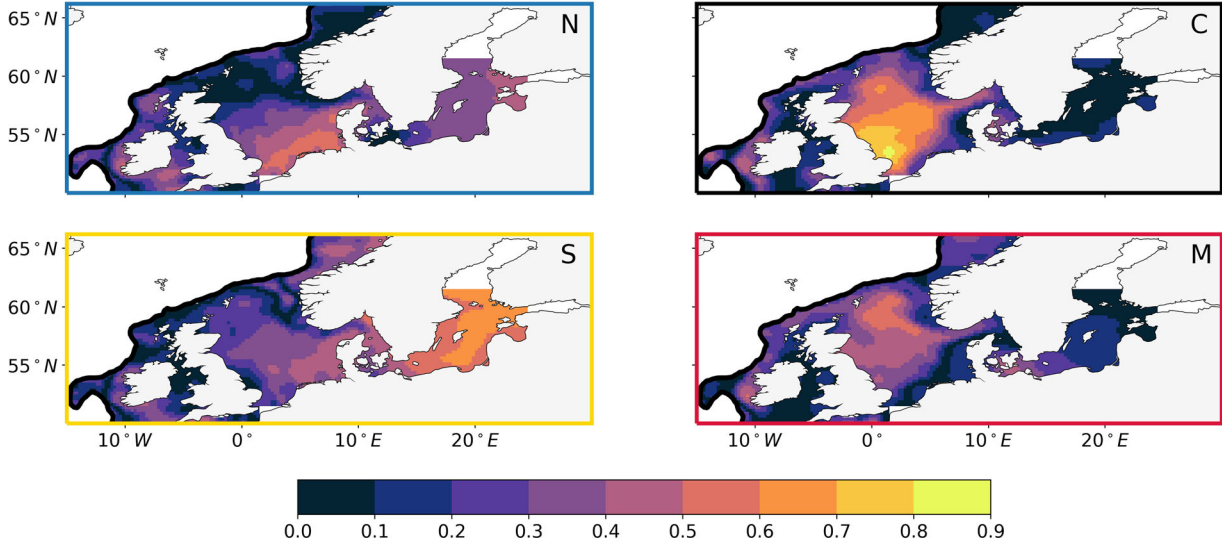


Fig. 5. Standardised maps of the composite of the daily sea level anomaly for each jet cluster: (N) Northern jet cluster, (C) Central jet cluster, (S) Southern jet cluster, (M) Mixed jet cluster. To standardise the maps in Fig. 4, we divide them by the standard deviation of the daily sea level anomaly over the 21-winter record. The grid points over the open ocean are masked and the continental shelf is delimited by the thick black line (the 500 m isobath).

describes a higher fraction of the SLA variability in the Baltic Sea than in the German Bight.

Additionally, one interesting message emerges for the Norwegian shelf. For the southern jet cluster, Fig. 5S shows similar values over the Norwegian shelf and in the German Bight. Therefore, even though the actual SLA over the Norwegian shelf is much smaller than in the German Bight (Fig. 4S), the southern jet cluster gives a similar contribution to sea level variability in the two regions.

3.3. Attribution of sea level variability

We now summarise the results in the previous sections by showing, into two maps, the jet clusters that are mostly associated with anomalously high and anomalously low SLA values across the northern European continental shelf. At each grid point, we compute the frequency of occurrence of the jet clusters during the days when the SLA is particularly high and during the days when it is particularly low. Then, at each grid point, we count the frequency of occurrence of the jet clusters on days when the SLA departs from the mean by more than -1.5 and by more than 1.5 standard deviations. In the end, we colour each grid point according to the frequency of occurrence of the jet clusters, to highlight the jet clusters that are most strongly associated with anomalous sea level values at that location (Fig. 6). If one of the jet clusters occurs at least 50% of time the SLA is anomalously high or low, the point is assigned to this jet cluster. If no

single jet cluster satisfies this condition, we consider all possible combinations of two jet clusters amounting to at least 50% frequency and assign the point to the combination with the highest frequency (see the caption of Fig. 6 for more information on the corresponding colours). If the frequency of occurrence associated with each combination is lower than 0.5, we colour the grid point grey.

The results in Fig. 6 mostly agree with those in Fig. 4, even though the former are partly contaminated by the SLA variability within each jet cluster. Both figures show that the Northern and Mixed jet clusters are important for anomalously high SLA values in the North Sea (Fig. 6A), and that the Central jet cluster is important for anomalously low SLA values in the North Sea (Fig. 6B). At the same time, however, anomalously low SLA values in the German Bight correspond both to the Central and the Southern jet clusters, despite the composite of the SLA for the Central jet cluster showing values close to zero in the region (Fig. 4). This suggests that, in the German Bight, over individual Central jet cluster events, the SLA can significantly depart from the composite value of the SLA associated with the Central jet cluster. We reach a similar conclusion for the Baltic Sea. In fact, Fig. 6 relates anomalously high SLA values to the Northern and the Mixed jet clusters, and anomalously low SLA values to the Southern and the Central jet clusters, even though Fig. 4 only associates the Northern and the Southern jet clusters with particularly high and low SLA values in the region. Over the Norwegian shelf, we only focus on the negative SLA values since Fig. 4 has already shown that positive values are not

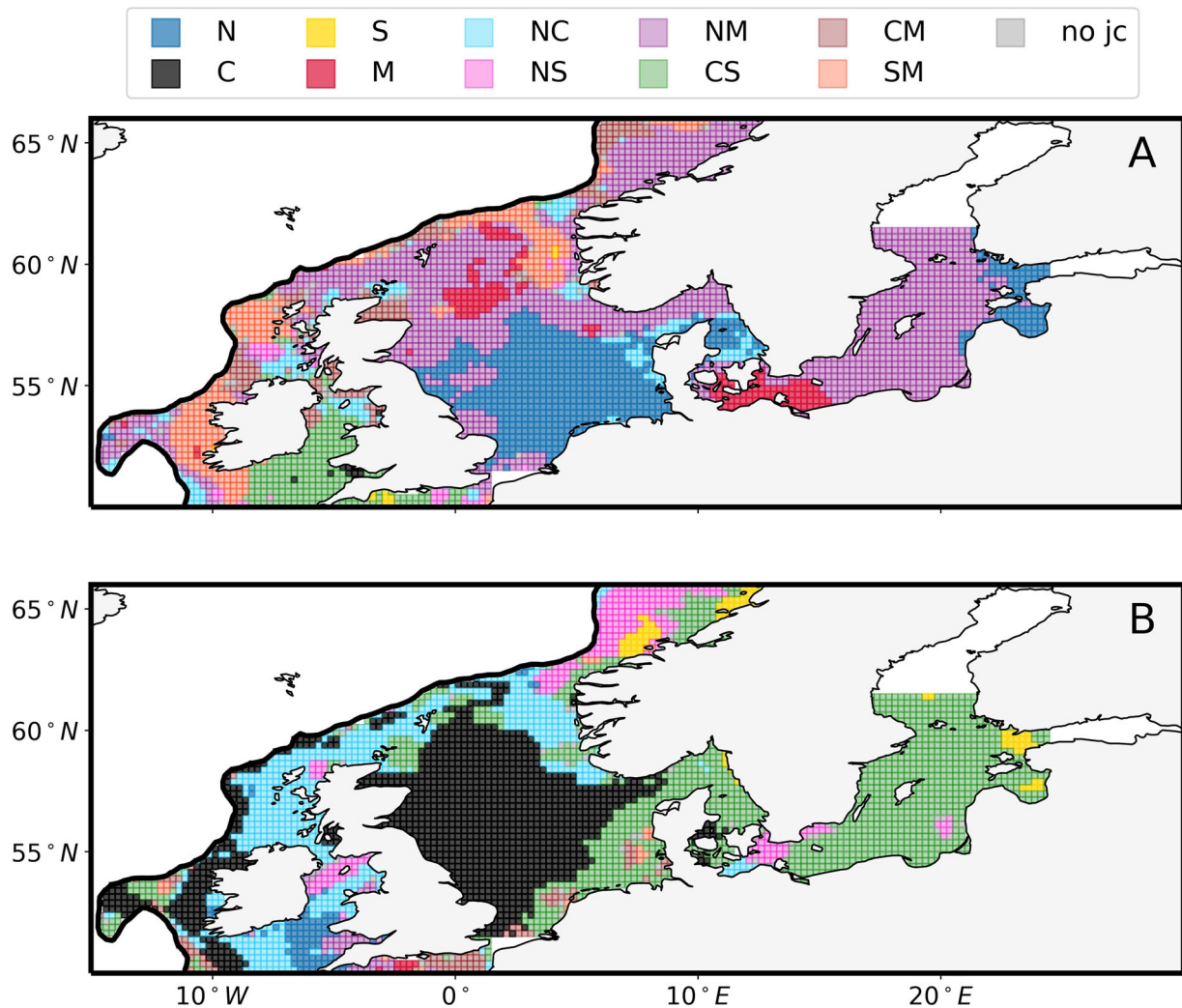


Fig. 6. Maps of jet clusters most strongly associated with anomalously high (A) and with anomalously low (B) sea level anomaly. Colours correspond to: Northern jet cluster (blue), Central jet cluster (black), Southern jet cluster (yellow), Mixed jet cluster (red), Northern and Central jet clusters (light blue), Northern and Southern jet clusters (lilla), Northern and Mixed jet clusters (purple), Central and Southern jet clusters (green), Central and Mixed jet clusters (brown), Southern and Mixed jet clusters (orange), otherwise ('no jc', grey). The grid points over the open ocean are masked and the continental shelf is delimited by the thick black line (i.e. the 500 m isobath).

clearly associated with any jet cluster. We note that Fig. 6 only partly agrees with Fig. 4. In fact, Fig. 6 shows that particularly low SLA values in the region correspond to the Northern, the Central, and the Southern jet clusters, even though we note that only the Southern jet cluster is associated with anomalously low SLA values over the entire Norwegian shelf.

4. Dynamic considerations

In this paper, we have adopted the jet cluster perspective of the winter-time atmospheric circulation in the North

Atlantic to document the contribution of local winds to the sea level variability over the northern European continental shelf. As a result, we have identified four patterns of SLA, each corresponding to a different configuration of the eddy-driven jet stream over the North Atlantic. In this section, we briefly discuss the dynamics of the ocean over the northern European continental shelf to investigate the role of local winds in driving the sea level patterns associated with each jet cluster. We start the discussion by identifying the main forces operating on the shelf. We conclude it by discussing the ability of the simple Ekman theory to explain the sea level patterns associated with each jet cluster.

Table 2. Magnitude of the depth-averaged Coriolis force, of the depth-averaged pressure gradient force and, of the depth-averaged force exerted by the winds, all averaged over the entire northern European continental shelf (more precisely, over the region of the shelf delimited by the coordinates 3°W–30°E and 51°N–66°N). Units are m s^{-2} .

	Coriolis force	Pressure gradient force	Force exerted by the winds
Northern jet cluster	1.7×10^{-6}	1.3×10^{-6}	2.0×10^{-6}
Central jet cluster	2.0×10^{-6}	1.5×10^{-6}	1.7×10^{-6}
Southern jet cluster	1.8×10^{-6}	1.7×10^{-6}	1.3×10^{-6}
Mixed jet cluster	1.7×10^{-6}	1.5×10^{-6}	1.4×10^{-6}

To describe the barotropic response of the ocean over the northern European continental shelf to each jet cluster, we use the depth-averaged momentum equation which, based on considerations found in previous studies, reduces to the balance of only three forces: the depth-averaged Coriolis force, the depth-averaged pressure gradient force and the depth-averaged force exerted by the winds. The ocean in the North Sea needs approximately two days to adjust to changes in the winds (e.g. Weenink, 1956; Pingree and Griffiths, 1980): since the jet clusters persist on average five days (Madonna et al., 2017), we expect the sea level pattern associated with each jet cluster (Fig. 4) to be approximately in steady state and, consequently, the term du/dt in the depth-averaged momentum equation to be negligible. Through scaling considerations, Pingree and Griffiths (1980) showed that the vertically averaged advection and bottom friction can also be neglected. Therefore, the depth-averaged momentum equation becomes:

$$f\hat{k} \times \mathbf{u} = -g\nabla(SLA) + \frac{1}{\rho_w \cdot H} \boldsymbol{\tau}_w \quad (3)$$

where the term on the left-hand side of Eq. (3) is the depth-averaged Coriolis force, the first term on the right-hand side is the depth-averaged pressure gradient force, and the second term is the depth-averaged force exerted by the wind stress; $f = 2\Omega \sin(\phi)$ is the Coriolis parameter, \hat{k} is the vertical unit vector, \mathbf{u} is the depth-averaged current, $g = 9.8 \text{ m s}^{-2}$ is the gravitational acceleration, ρ_w is the density of seawater, H is the water depth, and $\boldsymbol{\tau}_w$ is the wind stress.

It is not possible to simplify Eq. (3) further, as all three forces have similar magnitudes over the northern European continental shelf (Table 2). Table 2 shows, for each jet cluster, the magnitude of the depth-averaged Coriolis force, of the depth-averaged pressure gradient force, and of the depth-averaged force exerted by the winds, all averaged over the northern European continental shelf (more precisely, over the region of the shelf delimited by the coordinates 3°W–30°E and 51°N–66°N). We note that the three forces are comparable in magnitude on the shelf. This result is robust since we reach a

very similar conclusion when we compare the magnitude of the three forces at each grid point on the shelf (not shown).

Since both the wind stress term and the Coriolis force are important, the relationship between local winds and sea-level patterns associated with each jet cluster can be partly explained in terms of Ekman transport. To show its contribution, we compute the Ekman transport associated with each jet cluster and the rate of change of the sea level that it induces (Fig. 7). To calculate the Ekman transport, we use the formula for the volume transport generated by a stable wind blowing over an infinitely deep ocean (e.g. Gill, 1982; Cushman-Roisin and Beckers, 2010):

$$\mathbf{U}_{ek} = -\frac{1}{\rho_w f} \hat{k} \times \boldsymbol{\tau} \quad (4)$$

where \mathbf{U}_{ek} is the Ekman volume transport, ρ_w is the mean density (chosen equal to 1030 kg m^{-3}), f is the Coriolis parameter, \hat{k} is the vertical unit vector, and $\boldsymbol{\tau}$ is the wind stress at 10 m above the sea surface.

We find that Ekman transport explains well the sea level pattern associated with the Mixed jet cluster, it partly explains the sea level patterns associated with the Central and the Southern jet clusters, but it cannot explain the sea level pattern associated with the Northern jet cluster (Fig. 7). During Mixed jet cluster events, the anticyclonic winds over northern Europe cause water to converge into the middle and the northern parts of the North Sea and onto the Norwegian shelf (Fig. 7M). Indeed, the south-westerly winds over the Nordic Seas generate a south-eastward Ekman transport, whereas the easterly winds over the southern North Sea generate a northward Ekman transport. As a result, local winds drive water into the interior and the northern North Sea and, therefore, sustain the positive SLA in the region (Fig. 4M). Through Ekman transport, the winds over the Nordic Sea also push water onto the Norwegian shelf and, therefore, explain the positive SLA in the area. During Central jet cluster events, the southerly winds over the North Sea induce an eastward Ekman transport, which drives water from the UK to the coasts of

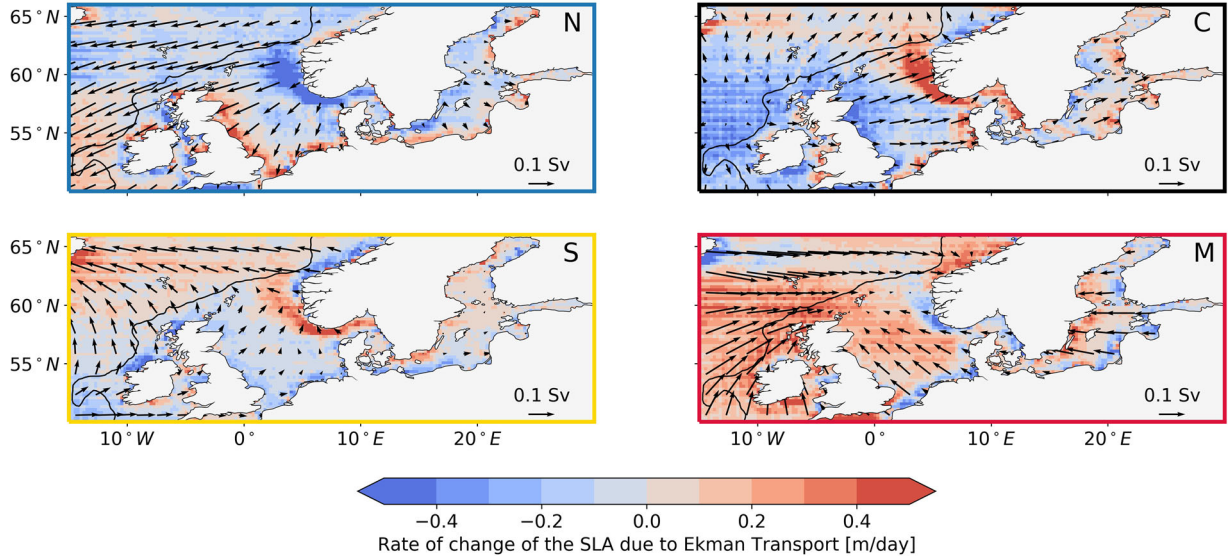


Fig. 7. Ekman transport associated with each jet cluster (arrows, $1 \text{ Sv} = 10^{-6} \text{ m}^3 \text{ s}^{-1}$) and rate of change of the sea level anomaly as a result of Ekman transport (m day^{-1}) for each jet cluster: (N) Northern jet cluster, (C) Central jet cluster, (S) Southern jet cluster, (M) Mixed jet cluster. Positive values indicate regions of convergence, whereas negative values indicate regions of divergence.

Denmark and Norway (Fig. 7C) and, therefore, explain the eastward sea level gradient in the basin (Fig. 4C). Similarly, during Southern jet cluster events, the easterly winds generate a northward Ekman transport, which pushes water into the open ocean and, in turn, decreases the sea level over the entire northern European continental shelf (Fig. 4S). As previously stated, Ekman transport does not explain all the features of the composite maps in Fig. 4 such as the meridional sea level gradient associated with the Northern jet cluster. As a possible explanation, we need to remember that the effects of the winds are highly affected by the bathymetry and the coastline geometry. As an example, Davies and Heaps (1980) showed how the presence of the Norwegian trench modifies the wind driven circulation and, therefore, the sea level pattern in the North Sea.

We would like to conclude this section with a note on the ocean circulation over the northern European continental shelf. By relating the wind stress, the SLA, and the depth-averaged currents, Eq. (3) suggests that the jet clusters might not only relate to sea level patterns, but also to ocean circulation patterns on the shelf (Fig. 1A). Figure 4 suggests this hypothesis: since the SLA gradient associated with each jet cluster is comparable with that of the mean ADT (Fig. 1A), the jet clusters could alter the geostrophic component of the circulation on the shelf. As an example, we note that the meridional SLA gradient associated with the Northern jet cluster is approximately half that of the mean ADT, meaning that the geostrophic component of the circulation in the North Sea might be strengthened by circa 50% during Northern jet cluster events.

5. Temporal relationship between the northern European sea level and the jet clusters

While in the previous sections, we have considered the spatial relationship between the northern European SLA and the jet clusters, we now address their temporal covariability at daily and monthly time scales. At first, we focus on the relationship at a few days' time scale, and we describe the evolution of the northern European SLA as the jet clusters persist for a few consecutive days. Then, we focus on the relationship at monthly time scale, and we assess to what extent the jet clusters reconstruct the monthly mean SLA variation over the northern European continental shelf.

5.1. Daily sea level evolution

The SLA from altimetry contains information on how the northern European sea level approaches equilibrium as the jet clusters persist for a few consecutive days. To analyse the adjustment process, we identify those cases when the jet clusters persist five days or longer and, for each jet cluster, we composite the SLA over the first and the fifth day of persistence, respectively (Fig. 8). We set the threshold at five days because we expect the northern European SLA to reach the equilibrium within this amount of time (e.g. Pingree and Griffiths, 1980; Saetre et al., 1988; Leppäranta and Myrberg, 2009) and also because it ensures a sufficiently large number of cases for a robust composite analysis (see Table 3).

Figure 8 shows a clear evolution of the SLA in relation to the Central and the Mixed jet clusters. If, on its first day

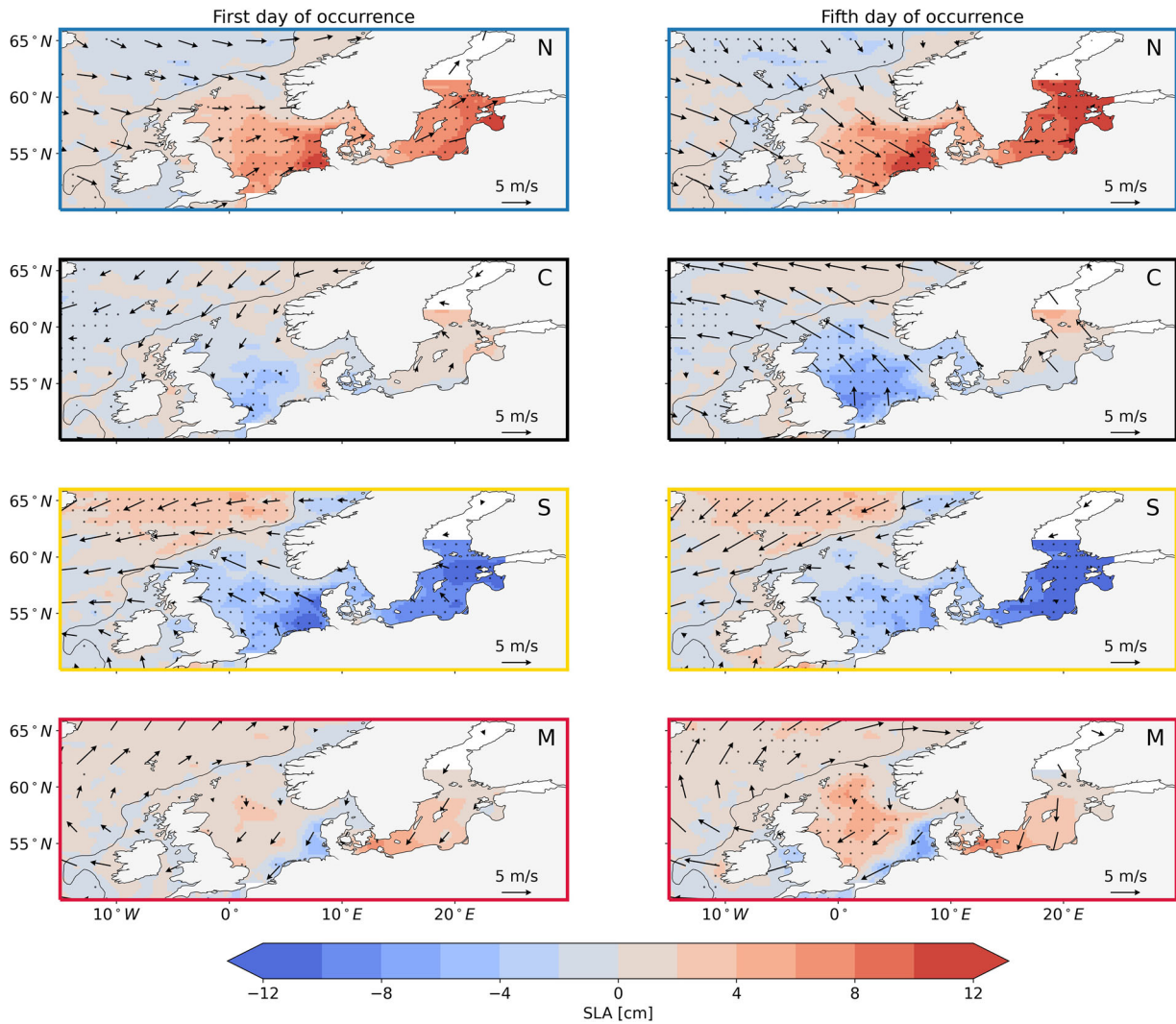


Fig. 8. Composite maps of daily sea level anomaly (shading, in cm) and 10 m wind anomaly (arrows, in m s^{-1}) over the first days (left column) and the fifth days (right columns) of persistence of each jet cluster: (N) Northern jet cluster, (C) Central jet cluster, (S) Southern jet cluster, (M) Mixed jet cluster. The black dots denote regions where the sea level anomaly composite is significantly different from zero at a 0.05 significance level. The grey line shows the location of the continental slope, depicted by the 500 m isobath.

of persistence, the Central jet cluster is associated with weak winds, on its fifth day of persistence, winds are southerly/south-easterly and their intensity exceeds 5 m s^{-1} over most of the continental shelf. Over the same period of time, the SLA drops by a few centimetres both in the western side and in the interior of the North Sea. Likewise, as the Mixed cluster persists for five consecutive days, the anti-cyclonic wind pattern over northern Europe intensifies, and the SLA rises in the interior of the North Sea.

On the contrary, the evolution of the SLA in relation to the Northern and the Southern jet clusters is less evident. We still see a slight increase of the SLA in the German Bight and the Baltic Sea during Northern jet cluster events and a few centimetres drop in the Baltic Sea during Southern jet cluster events. However, contrary

to our expectations, the SLA in the German Bight rises as the Southern jet cluster persists for a few consecutive days. Moreover, on their first day of occurrence, both jet clusters are already associated with well developed SLA patterns.

5.2. Interannual sea level variability

The atmospheric circulation over Europe is linked to the configuration of the jet stream over the North Atlantic (e.g. Madonna et al., 2017). Therefore, we expect the frequency of occurrence of different jet configurations to explain part of the monthly mean sea level variability over the northern European continental shelf. To estimate the strength of this relationship, at each grid point of the

Table 3. Number of cases when each jet cluster persists at least five consecutive days.

	Northern jet cluster	Central jet cluster	Southern jet cluster	Mixed jet cluster
Number of cases	38	32	28	43

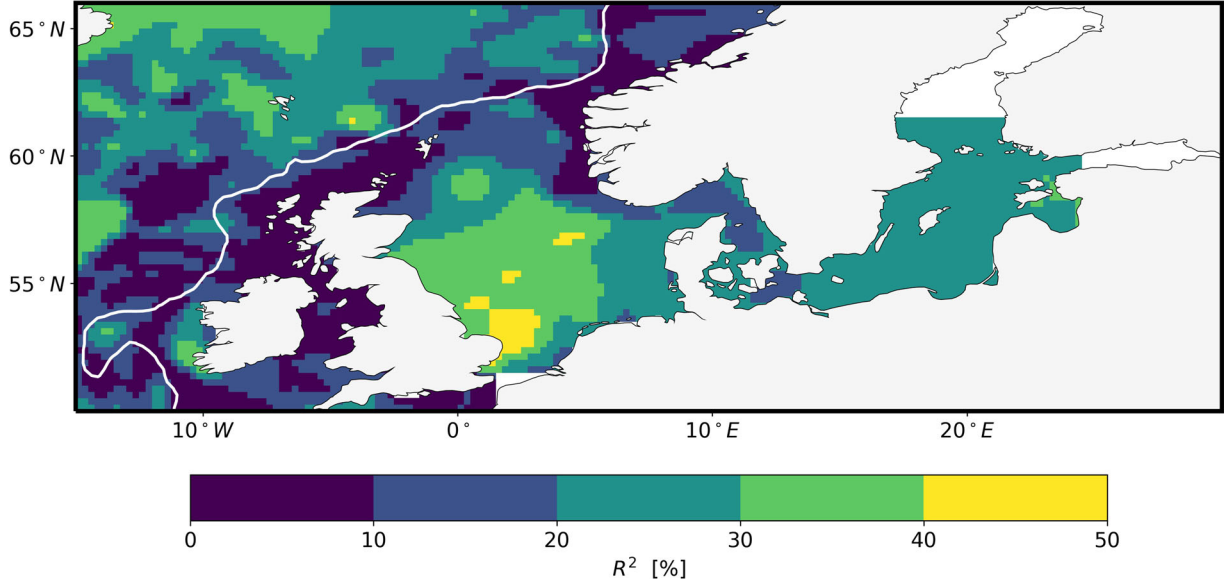


Fig. 9. At each grid point, fraction of the monthly mean sea level anomaly variance in winter that is explained by the multiple linear regression model.

northern European continental shelf, we build the following multiple linear regression model:

$$SLA = a + b \cdot freq_N + c \cdot freq_C + d \cdot freq_S + e \cdot freq_M \quad (5)$$

where SLA is the monthly mean SLA in winter, and $freq_N$, $freq_C$, $freq_S$, $freq_M$ are the monthly frequency of occurrence of the Northern, the Central, the Southern, and the Mixed jet clusters. We expect the regression model based on the jet clusters to explain a lower fraction of the monthly mean SLA variance when compared to a model based on the EOFs since this, by design, would maximise the explained variance of the SLA. However, the model above is still valuable: it can help quantify the contribution of the wind direction to the northern European sea level variability since the jet clusters determine the spatial pattern of the daily wind field over the North Atlantic, rather than its intensity.

Figure 9 shows that the temporal co-variability between the jet clusters and the northern European sea level varies considerably over the northern European continental shelf. We find the strongest covariance in the interior and in the western part of the North Sea, where the model explains between 40 and 50% of the SLA variance. The fraction of the variance explained by the model decreases in the Baltic Sea and the eastern part of the

North Sea, where it mostly ranges between 20 and 30%, and reaches its lowest values in the Norwegian Trench, over the Norwegian shelf and along the continental slope, where it does not exceed 20%.

6. Conclusions and outlook

The jet cluster approach helps identify a number of locations ($\sim 40\%$ of the northern European continental shelf) where a single jet cluster induces either high or low sea level values and therefore sheds new lights on the atmospheric control on the North European sea level. For example, negative SLA values along the east coast of England are mainly associated with the Central jet cluster, whereas positive SLA values in the German Bight are mainly associated with the Northern jet cluster. The case of the German Bight offers an interesting comparison with Dangendorf et al. (2014), who used both a correlation map and a composite analysis approach to determine the single atmospheric pattern responsible for anomalously high sea level values in the region. Indeed, we note that the approach based on the jet clusters and the one developed by Dangendorf et al. (2014) return partly different results: while the spatial structure of the atmospheric pattern in Dangendorf et al. (2014) resembles the Northern jet cluster, its centres of actions are located

eastward with respect to those of the Northern jet cluster (Fig. 3N). This discrepancy might result from the linear regression approaches mixing different jet clusters since high sea level in the German Bight is not uniquely associated with the Northern jet cluster. An additional study that focuses on the sea level variations in the German Bight could help clarify whether the atmospheric index by Dangendorf et al. (2014) is accurate enough to reconstruct the wind component of the sea level variability in the region.

In other parts of the shelf, the sea level responds to more than one jet cluster. In Fig. 4, we note that positive SLA values along the east coast of England are associated with both the Northern and the Mixed jet clusters. Similarly, in the interior of the North Sea, negative SLA values are associated with both the Southern and the Central jet clusters. In addition, Fig. 6 shows that, in the Baltic Sea, anomalously low sea level values are associated with both the Southern and the Central jet clusters, whereas positive sea level values are associated with both the Northern and the Mixed jet clusters. Therefore, even though a composite analysis would return a single atmospheric pattern associated with either high or low sea level at these locations, this would not correspond to any typical atmospheric condition since it would result from a combination of several jet clusters.

The jet cluster approach can only partly describe the evolution and adjustment of northern European sea level to wind variations over the North Atlantic and northern Europe. In this regard, while the Central and the Mixed jet clusters are associated with an intuitive evolution of the northern European SLA, with the corresponding SLA patterns intensifying with the days of persistence, the Northern and the Southern jet clusters are not. Indeed, the SLA patterns associated with the Northern and the Southern jet clusters already reach the equilibrium on the first day of occurrence.

Considering longer timescales, the jet clusters framework provides new insights on the contribution of the winds to interannual sea level variability over the northern European continental shelf. Applying a multiple linear regression model, we show that the jet clusters can explain up to 50% of the SLA variance. The explained variance varies regionally and suggests that in some regions (e.g. the interior and western side of the North Sea), the large-scale flow (i.e. the wind direction) rather than the strength of the winds (i.e. the wind speed) affects the SLA variability, but further studies are required to investigate this in more details.

Future works might further explore the relationship between the jet clusters and the ocean circulation over the northern European continental shelf. An in-depth investigation of the link between the jet clusters and the two

EOFs of surface circulation identified by Kauker and von Storch (2000) would be a follow-up of this study. In addition, the jet cluster perspective suggests that approximately 25% of the winter days are characterised by blocking conditions over northern Europe. We believe that a reference study that describes the ocean response to an anticyclonic wind pattern over northern Europe would be of interest since, to the authors' knowledge, it does not exist. Finally, the jet clusters could also be used to extend the work by Winther and Johannessen (2006), who used the NAO to investigate the atmospheric contribution to the exchange of water between the open-ocean and the North Sea. However, the NAO explains only a fraction of the atmospheric variability in the North Atlantic and might give an incomplete description of the atmospheric contribution to inflow and outflow of the northern European continental shelf. The jet clusters might provide a more complete and more realistic description of the exchange of water between the Nordic Seas and the shelf since they represent physical patterns of the atmosphere.

Acknowledgements

This study has been conducted using E.U. Copernicus Marine Service Information and the ERA-Interim reanalysis dataset provided by the European Centre for Medium-Range Weather Forecasts. The authors would like to thank an anonymous reviewer for the comments and suggestions, which improved the quality of the manuscript.

Disclosure statement

No potential conflict of interest was reported by the authors.

Funding

Fabio Mangini is funded with an institute fellowship of the Research Council of Norway (contract no. 272411/F40). This work was also supported by the Research Council of Norway project jetSTREAM (231716) and by the Climate Hazards and EXtremes (CHEX) project of the Bjerknes Centre from Climate Research. To conclude, Léon Chafik acknowledges support from the Swedish National Space Agency through the FiNNESS project (Dnr: 133/17).

Supplemental data

Supplemental data for this article can be accessed [here](#).

References

- Barrier, N., Treguier, A. M., Cassou, C. and Deshayes, J. 2013. Impact of the winter north-atlantic weather regimes on subtropical sea-surface height anomaly. *Clim. Dyn.* **41**, 1159–1171. doi:10.1007/s00382-012-1578-7
- Barrier, N., Cassou, C., Deshayes, J. and Treguier, A. M. 2014. Response of North Atlantic circulation to atmospheric weather regimes. *J. Phys. Oceanogr.* **44**, 179–201. doi:10.1175/JPO-D-12-0217.1
- Bentamy, A., Grodsky, S. A., Elyouncha, A., Chapron, B. and Desbiolles, F. 2017. Homogenization of scatterometer wind retrievals. *Int. J. Climatol.* **37**, 870–889. doi:10.1002/joc.4746
- Cassou, C., Minvielle, M., Terray, L. and Périgaud, C. 2011. A statistical-dynamical scheme for reconstructing ocean forcing in the atlantic. Part I: weather regimes as predictors for ocean surface variables. *Clim. Dyn.* **36**, 19–39. doi:10.1007/s00382-010-0781-7
- Cazenave, A., Meyssignac, B., Ablain, M., Balmaseda, M., Bamber, J. and co-authors. 2018. Global sea-level budget 1993-present. *Earth Syst. Sci. Data* **10**, 1551–1590.
- Chafik, L., Nilsen, J. E. Ø. and Dangendorf, S. 2017. Impact of North Atlantic teleconnection patterns on northern European sea level. *JMSE*. **5**, 43. doi:10.3390/jmse5030043
- Cushman-Roisin, B. and Beckers, J. M. 2010. *Introduction to Geophysical Fluid Dynamics. Physical and Numerical Aspects*. Vol. **101**. Academic Press, Cambridge, Massachusetts.
- Dangendorf, S., Wahl, T., Hein, H., Jensen, J., Mai, S. and co-authors. 2012. Mean sea level variability and influence of the North Atlantic oscillation on long-term trends in the German Bight. *Water* **4**, 170–195. doi:10.3390/w4010170
- Dangendorf, S., Wahl, T., Nilson, E., Klein, B. and Jensen, J. 2014. A new atmospheric proxy for sea level variability in the southeastern North Sea: observations and future ensemble projections. *Clim. Dyn.* **43**, 447–467. doi:10.1007/s00382-013-1932-4
- Davies, A. M. and Heaps, N. S. 1980. Influence of the Norwegian Trench on the wind-driven circulation of the North Sea. *Tellus* **32**, 164–175.
- Dee, D. P., Uppala, S. M., Simmons, A. J., Berrisford, P., Poli, P. and co-authors. 2011. The ERA-Interim reanalysis: configuration and performance of the data assimilation system. *QJR Meteorol. Soc.* **137**, 553–597. doi:10.1002/qj.828
- Gill, A. 1982. *Atmosphere-Ocean Dynamics*. Elsevier, New York.
- Hurrell, J. W. 1995. Decadal trends in the North Atlantic oscillation: Regional temperatures and precipitation. *Science* **269**, 676–679. doi:10.1126/science.269.5224.676
- Jevrejeva, S., Moore, J. C., Woodworth, P. L. and Grinsted, A. 2005. Influence of large-scale atmospheric circulation on European sea level: results based on the wavelet transform method. *Tellus A* **57**, 183–193. doi:10.3402/tellusa.v57i2.14609
- Kauker, F. and von Storch, H. 2000. Statistics of “Synoptic Circulation Weather” in the North Sea as derived from a multiannual OGCM simulation. *J. Phys. Oceanogr.* **30**, 3039–3049. doi:10.1175/1520-0485(2000)030<3039:SOSCWI>2.0.CO;2
- Lamb, H. H. and Frydendahl, K. 1991. *Historic Storms of the North Sea, British Isles and Northwest Europe*. Cambridge University Press, Cambridge.
- Leppäranta, M. and Myrberg, K. 2009. *Physical Oceanography of the Baltic Sea*. Springer-Verlag, Berlin-Heidelberg-New York.
- Li, C. and Wettstein, J. J. 2012. Thermally driven and eddy-driven jet variability in reanalysis. *J. Clim.* **25**, 1587–1596. doi:10.1175/JCLI-D-11-00145.1
- Madonna, E., Li, C. and Wettstein, J. J. 2019. Suppressed eddy driving during southward excursions of the north atlantic jet on synoptic to seasonal time scales. *Atmos. Sci. Lett.* **20**, 1–11. doi:10.1002/asl.937.
- Madonna, E., Li, C., Grams, C. M. and Woollings, T. 2017. The link between eddy-driven jet variability and weather regimes in the North Atlantic-European sector. *QJR Meteorol. Soc.* **143**, 2960–2972. doi:10.1002/qj.3155
- Michelangeli, P. A., Vautard, R. and Legras, B. 1995. Weather regimes: recurrence and quasi stationarity. *J. Atmos. Sci.* **52**, 1237–1256. > 2.0.CO;2. doi:10.1175/1520-0469(1995)052<1237:WRRASQ>2.0.CO;2
- Pingree, R. D. and Griffiths, D. K. 1980. Currents driven by a steady uniform wind stress on the shelf seas around the british-isles. *Oceanol. Acta* **3**, 227–236.
- Pujol, M.-I., Faugère, Y., Taburet, G., Dupuy, S., Pelloquin, C. and co-authors. 2016. DUACS DT2014: the new multi-mission altimeter data set reprocessed over 20 years. *Ocean Sci.* **12**, 1067–1090. doi:10.5194/os-12-1067-2016
- Richter, K., Nilsen, J. E. Ø. and Drange, H. 2012. Contributions to sea level variability along the Norwegian coast for 1960–2010. *J. Geophys. Res.* **117**, 1–12. doi:10.1029/2011JC007826.
- Saetre, R., Aure, J. and Ljøen, R. 1988. Wind effects on the lateral extension of the Norwegian Coastal water. *Cont. Shelf Res.* **8**, 239–253. doi:10.1016/0278-4343(88)90031-3
- Vautard, R. 1990. Multiple weather regimes over the North Atlantic: analysis of precursors and successors. *Mon. Wea. Rev.* **118**, 2056–2081. MWROTN)2.0.CO;2. doi:10.1175/1520-0493(1990)118<2056:MWROTN>2.0.CO;2
- Wahl, T., Haigh, I. D., Woodworth, P. L., Albrecht, F., Dillingh, D. and co-authors. 2013. Observed mean sea level changes around the North Sea coastline from 1800 to present. *Earth Sci. Rev.* **124**, 51–67. doi:10.1016/j.earscirev.2013.05.003
- Wakelin, S. L., Woodworth, P. L., Flather, R. A. and Williams, J. A. 2003. Sea-level dependence on the NAO over the NW European continental shelf. *Geophys. Res. Lett.* **30**, 1403.
- Weenink, M. P. 1956. The “twin” storm surges during 21st–24th December, 1954. A case of resonance. *Dtsch. Hydrogr. Z.* **9**, 240–249. doi:10.1007/BF02020089
- Winther, N. G. and Johannessen, J. A. 2006. North Sea circulation: Atlantic inflow and its destination. *J. Geophys. Res.* **111**, 1–12, doi:10.1029/2005JC003310.
- Xie, J., Bertino, L., Counillon, F., Lisaeter, K. A. and Sakov, P. 2017. Quality assessment of the TOPAZ4 reanalysis in the Arctic over the period 1991–2013. *Ocean Sci.* **13**, 123–144. doi:10.5194/os-13-123-2017
- Yan, Z., Tsimplis, M. N. and Woolf, D. 2004. Analysis of the relationship between the North Atlantic oscillation and sea-level changes in northwest Europe. *Int. J. Climatol.* **24**, 743–758. doi:10.1002/joc.1035